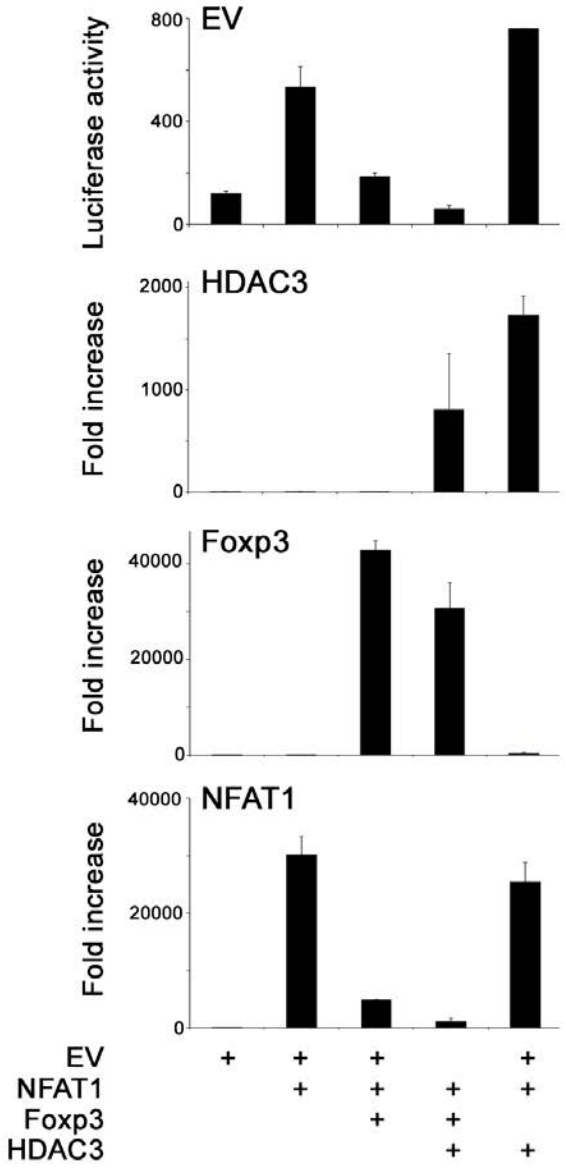

Suppl. Fig. 1 IL-2 luciferase activity (mean ± SD) and gene expression after viral transfection of 293T cells with HDAC3, Foxp3 and NFAT1 or empty vector (EV).

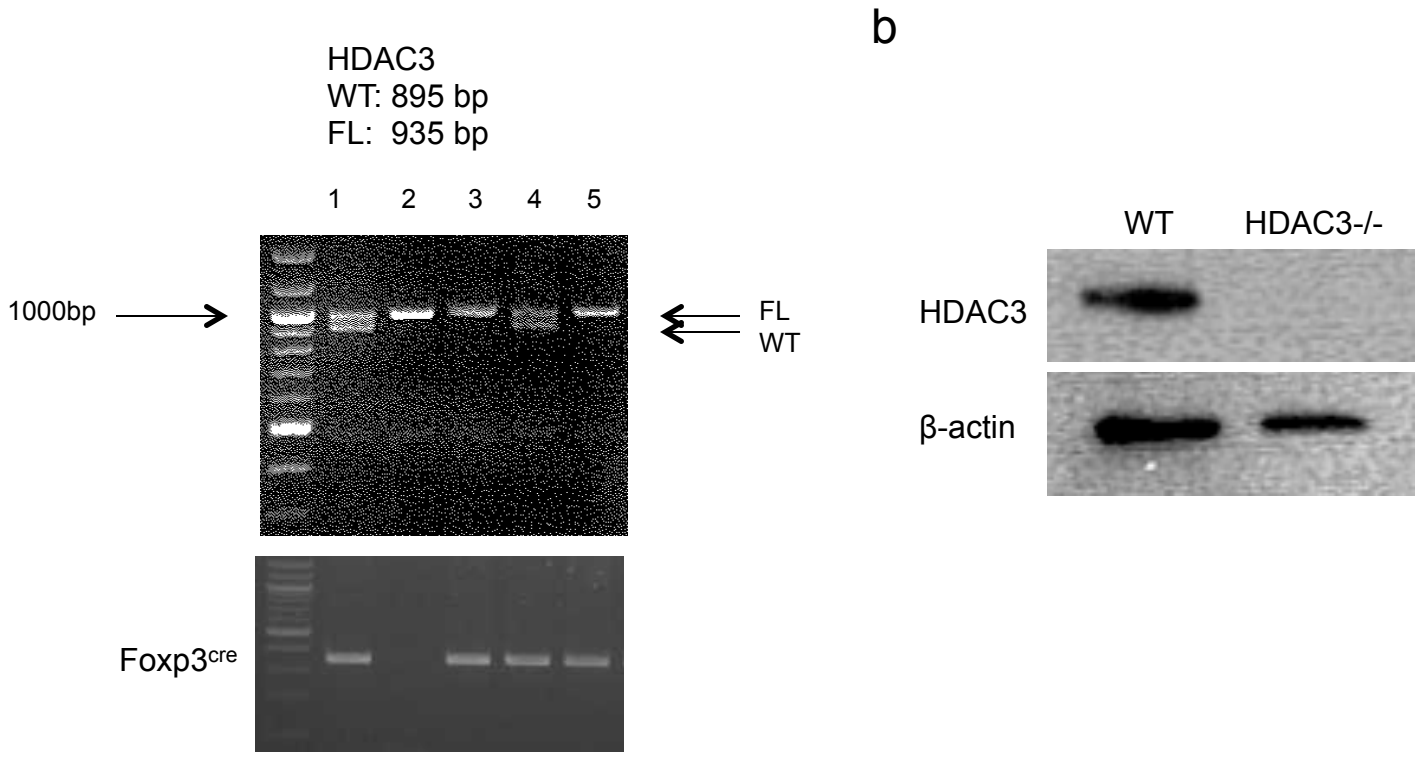

Suppl. Fig. 2 a) Mice with conditional *Hdac3* deletion in their Foxp3+ Tregs were generated by breeding floxed HDAC3 and Foxp3cre mice; HDAC3 FL/FL and Foxp3cre positive are seen in lanes 3 and 5. b) Confirmation of HDAC3 deletion in cell-sorted YFP+ Foxp3+ Treg cells by Western blotting.

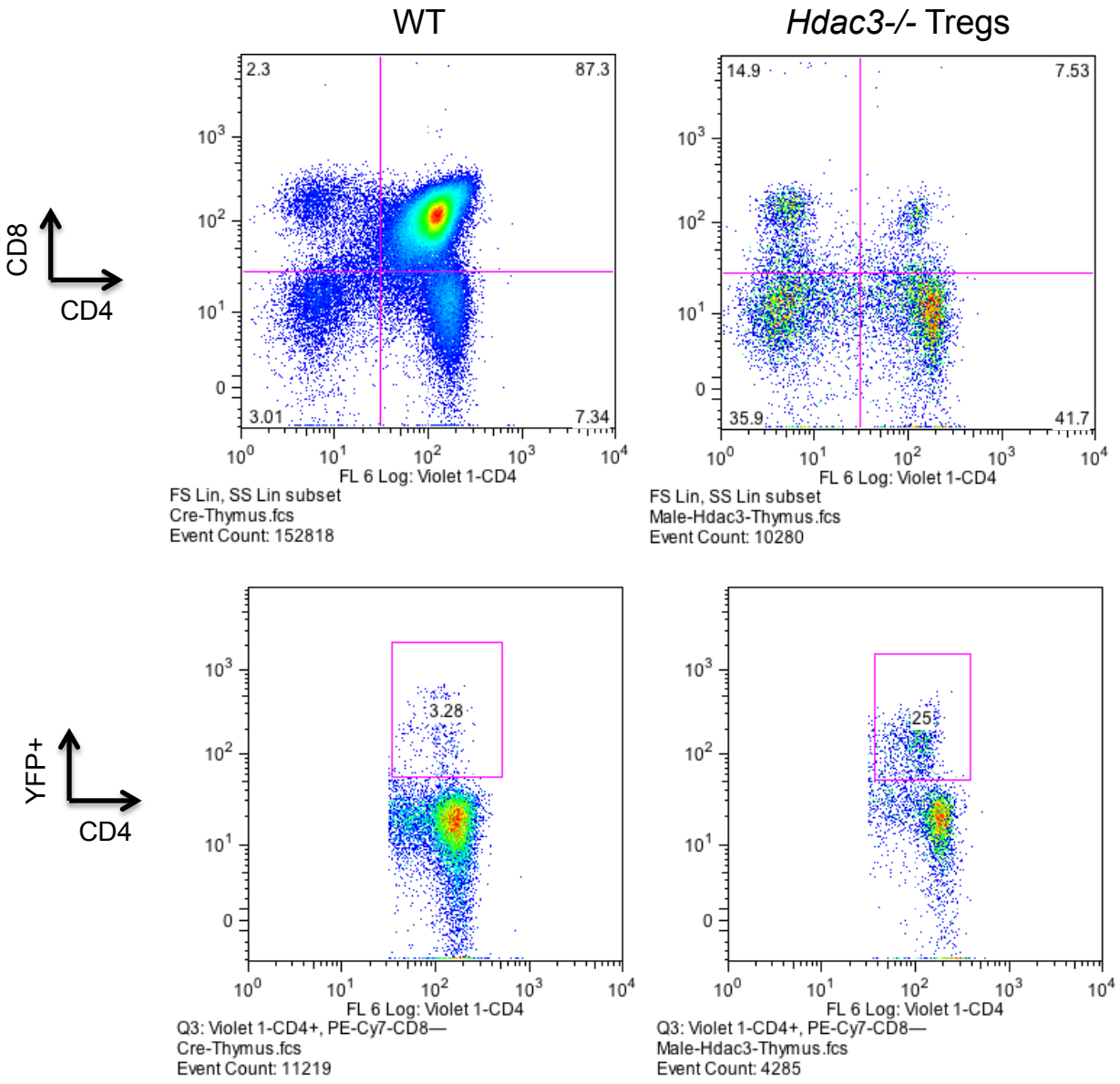

Suppl. Fig. 3 Analysis of thymic T cell development by flow cytometry showed that *Hdac3* deletion in Tregs was associated with decreased double-positive thymocytes and increased single positive cells, as well as an increased proportion of YFP+ (Foxp3+) Treg cells; data are representative of 4 mice/group.

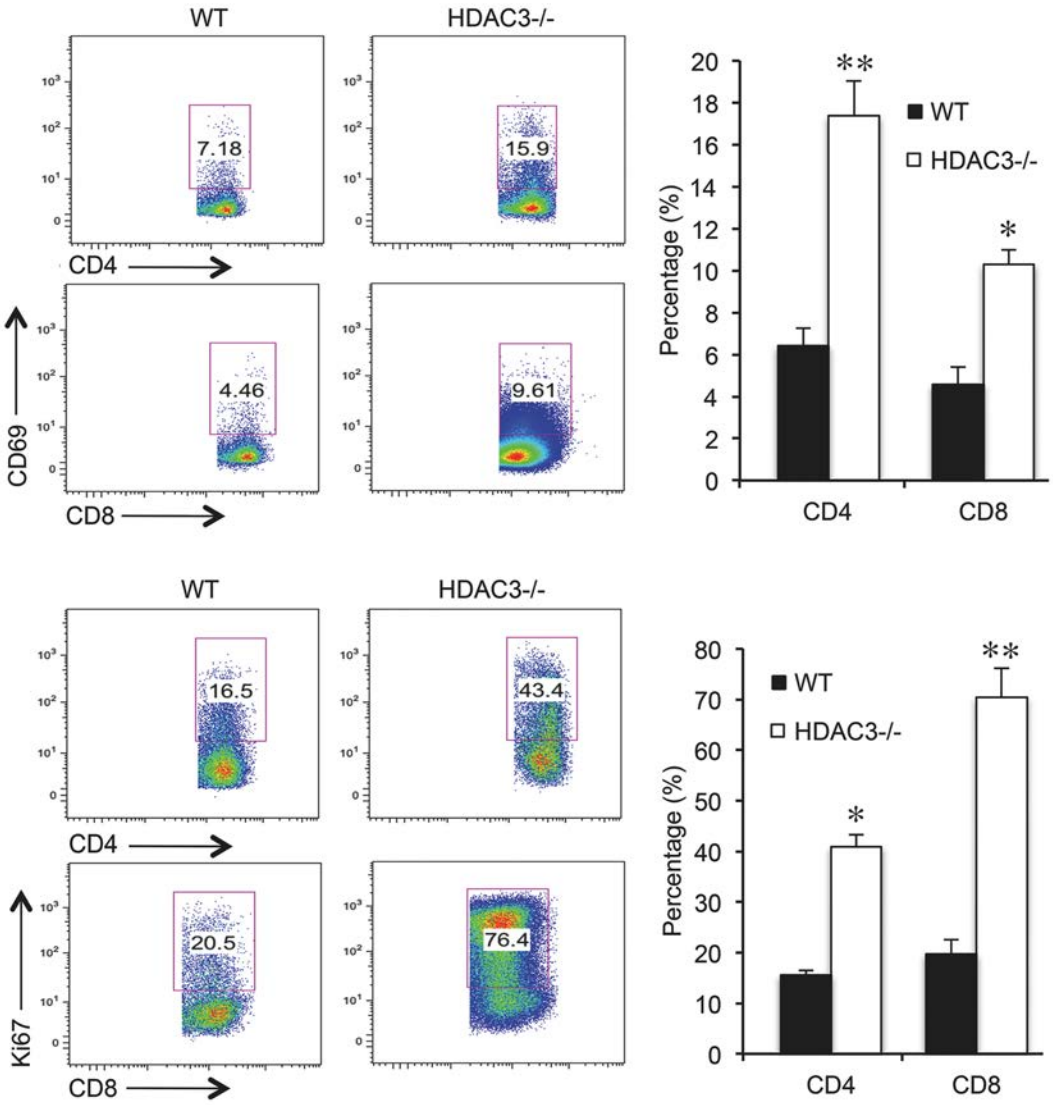

Suppl. Fig. 4 *Hdac3* deletion in Tregs was associated with increased CD4 and CD8 T cell activation, as shown by increased proportions and absolute numbers of CD4+CD69^{hi} and CD8+CD69^{hi} cells, and also CD4+Ki67+ and CD8+Ki67+ proliferating T cells (pooled LN and spleen cells); mean ± SD, 4/group, *p<0.05 and **p<0.01 vs. WT using unpaired Student's t-test.

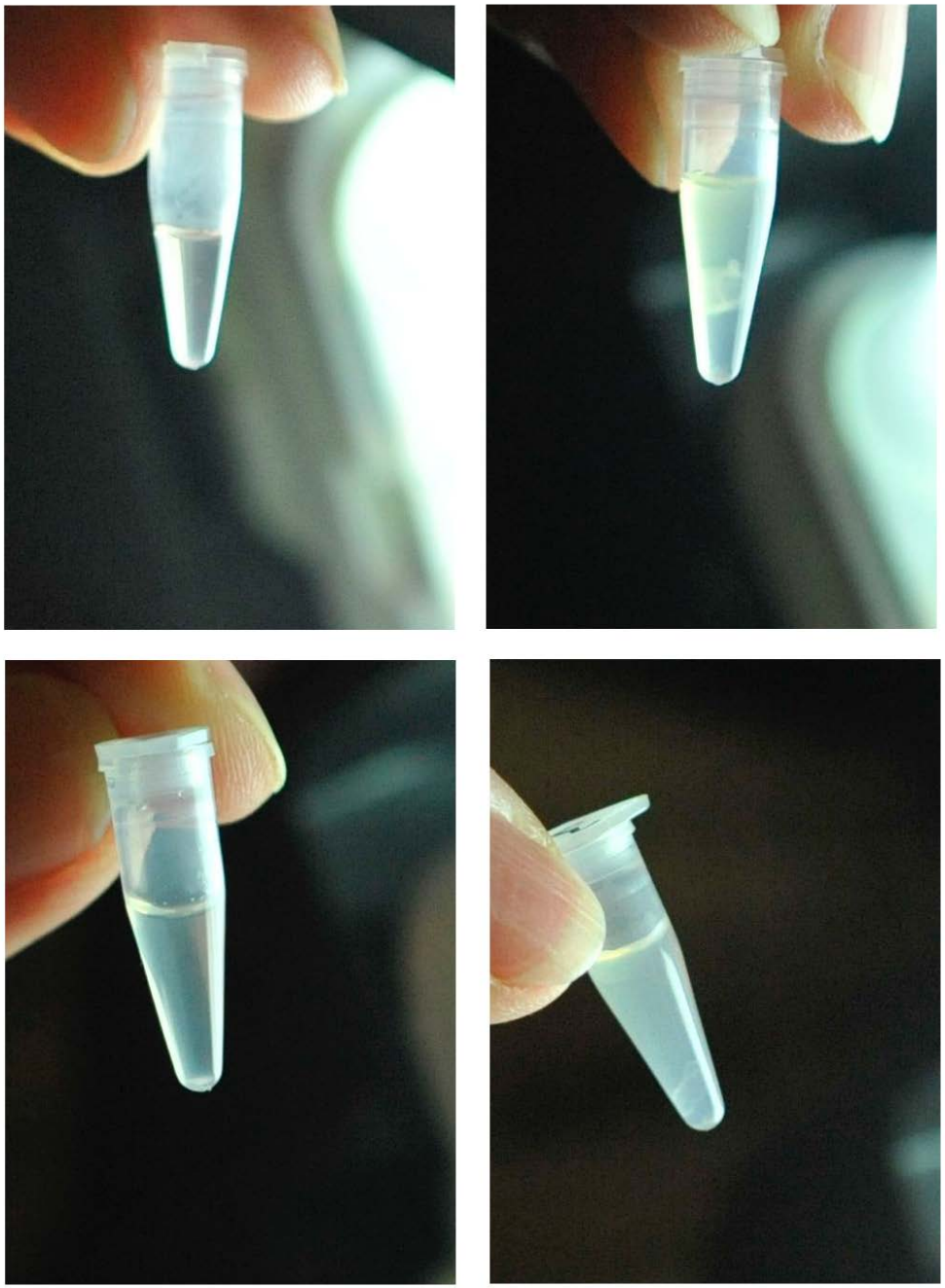

Suppl. Fig. 5 Cryoglobulin production in mice whose Tregs lack *Hdac3*; an example of plasma from a 4 week old male mouse is shown, and representative of 8 mice/ group studied.

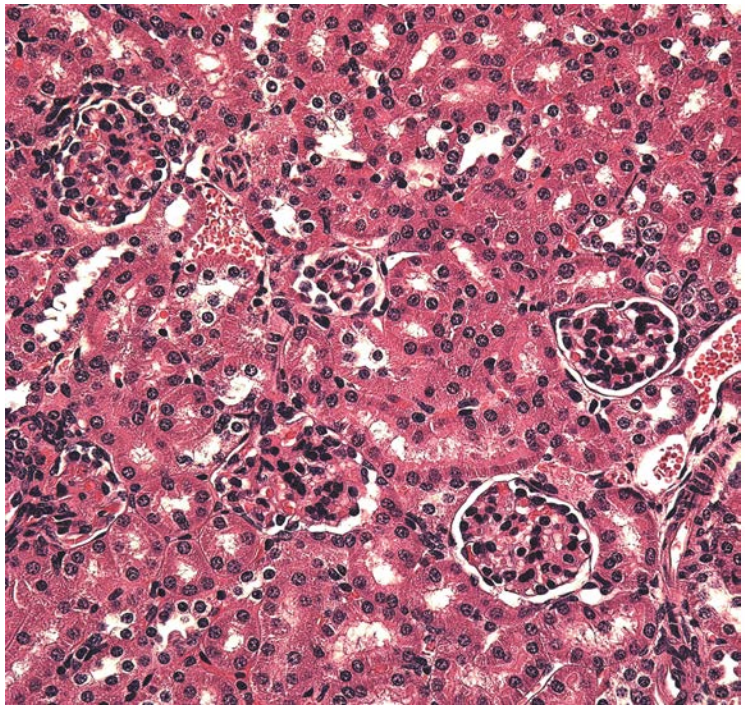

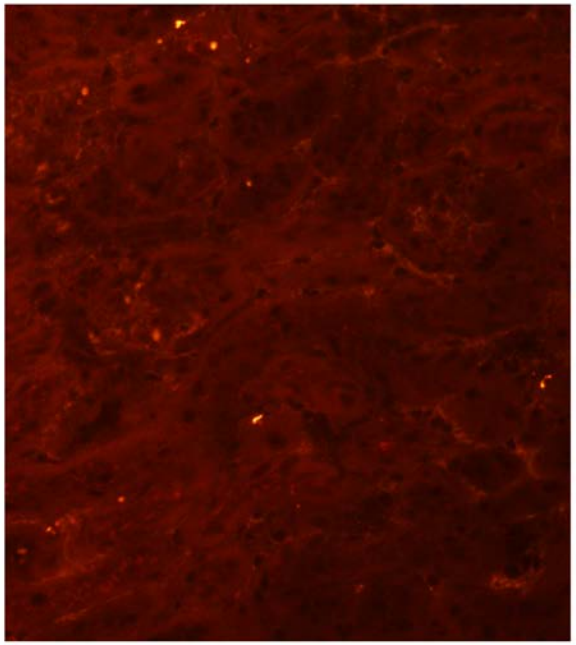

WT kidney, anti-IgM abs, 1:200

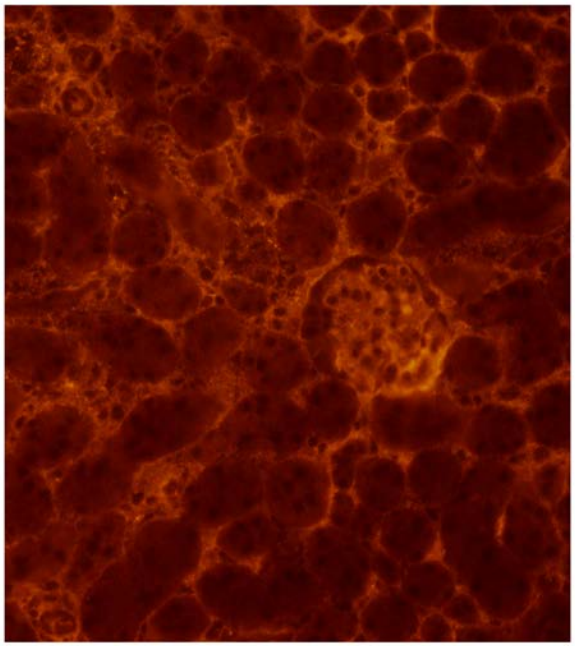

HDAC3-Foxp3 Cre kidney, anti-IgM abs, 1:200

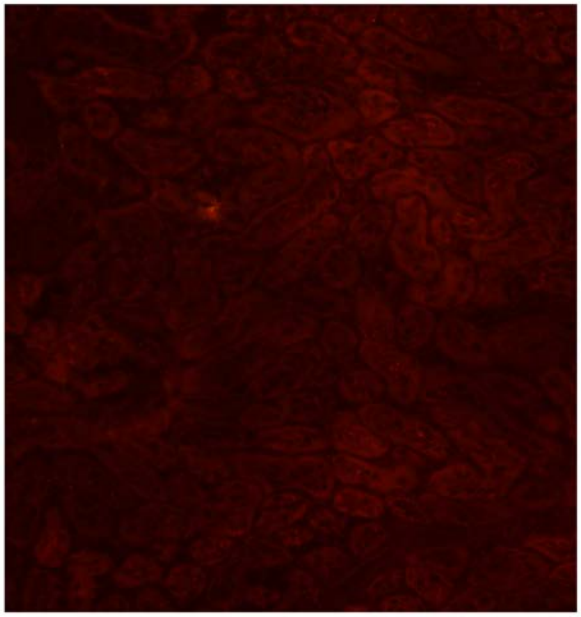

WT kidney, anti-Ly6G abs, 1:50

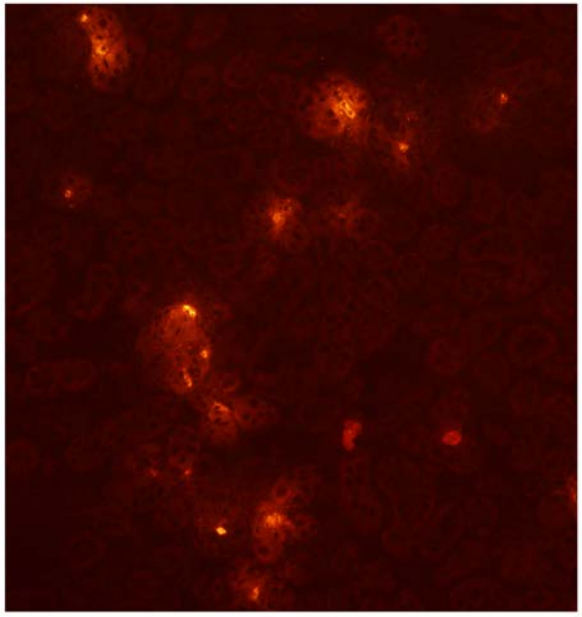

HDAC3-Foxp3 Cre kidney, anti-Ly6G abs, 1:50

Suppl. Fig. 6 HDAC3-Foxp3 Cre KO mice develop a proliferative immune complex glomerulonephritis; note hypercellular glomeruli, with IgM deposition and neutrophil infiltration, in a 4 week old male mouse, representative of 8 mice/group studied (original magnifications x400).

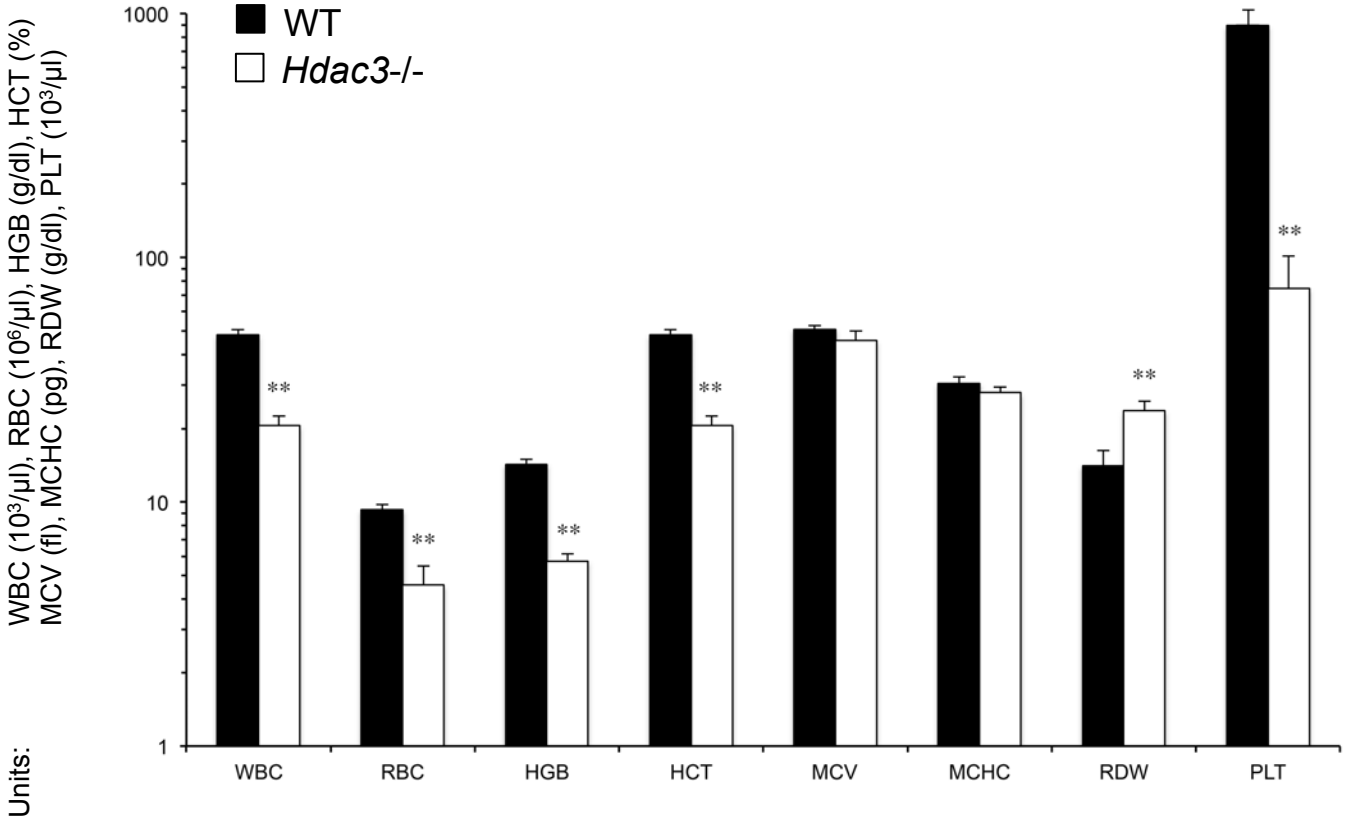

Suppl. Fig. 7 Hematologic parameters in *Hdac3-/-* vs. WT controls, involving 4 mice/ group, 4 wks of age; data are mean ± SD, with analysis by Student's t-test, *p<0.05, **p<0.01 vs. WT).

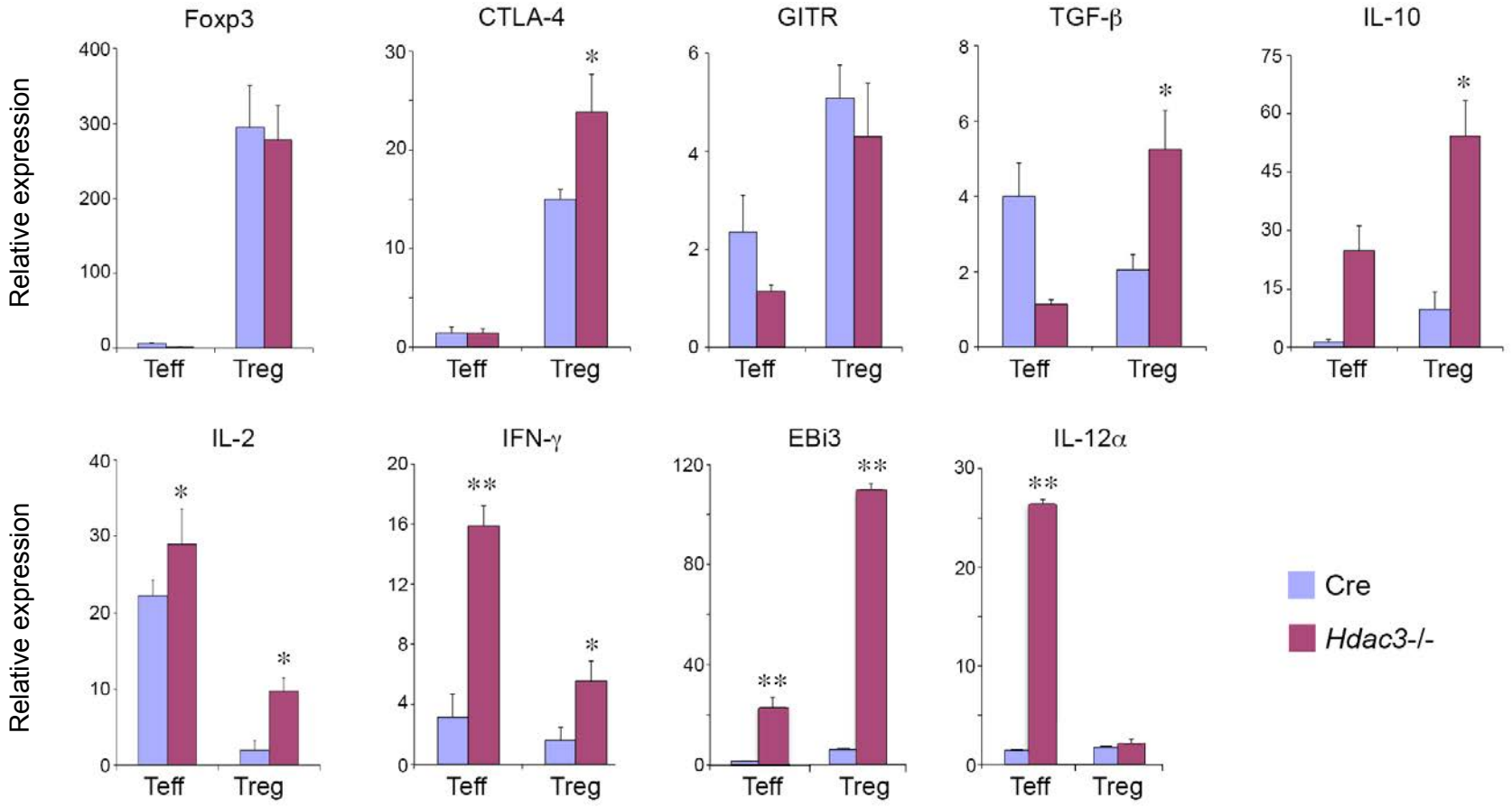

Suppl. Fig. 8 qPCR analysis of YFP-sorted Tregs from WT or *Hdac3*-/- mice (4 weeks of age); data are mean ± SD of 4 mice/group, with *p<0.05, **p<0.01(Student's t-test) for gene expression between corresponding cell populations.

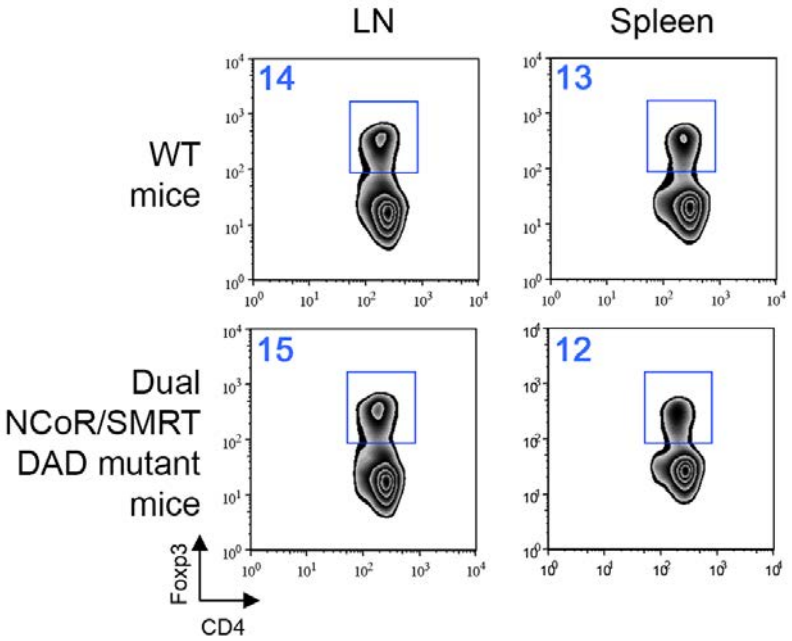

Suppl. Fig. 9 Male mice (6-8 weeks) with dual mutations of the NCoR and SMRT DAD sites had normal proportions of CD4+Foxp3+ Tregs in their lymph nodes and spleens; data are representative of 3 mice/group.

CD4 T cell proliferation

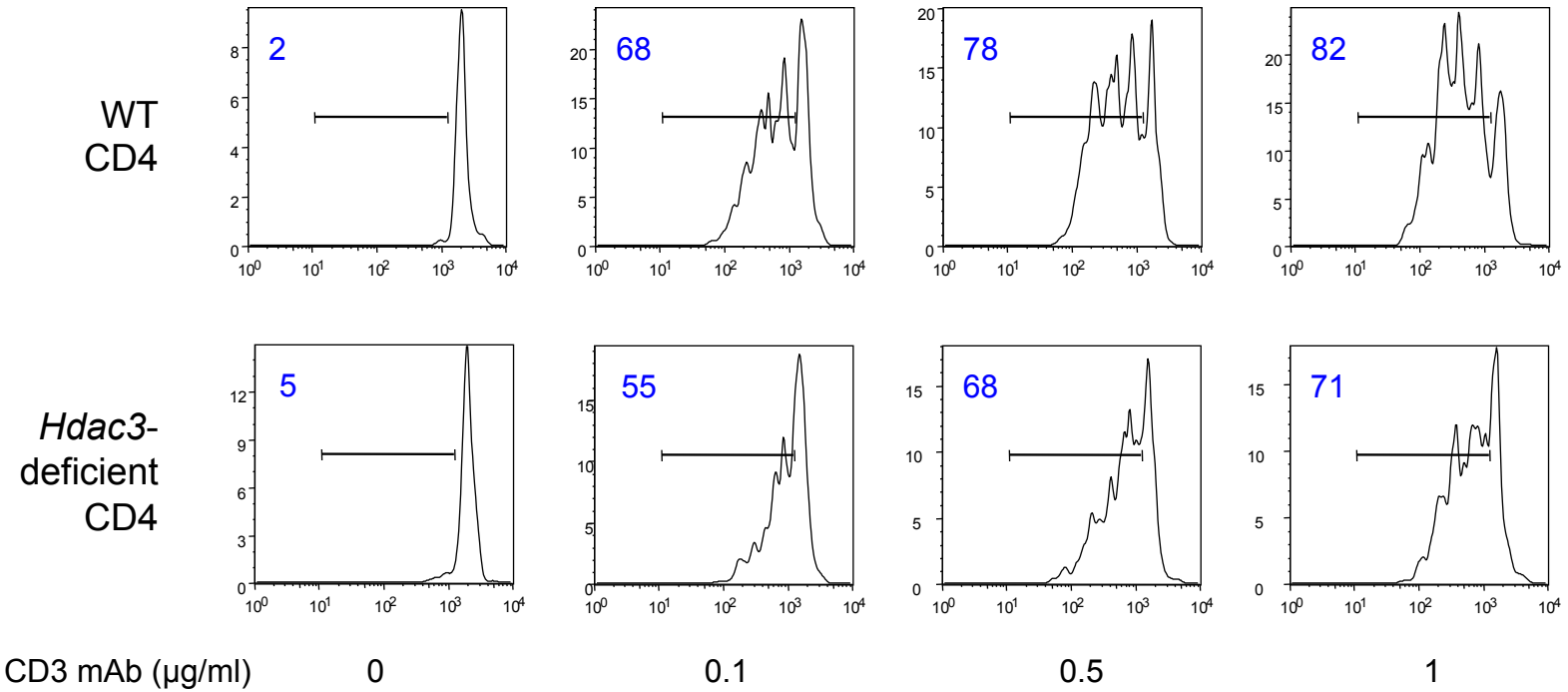

Suppl. Fig. 10 CD3 mAb-induced T cell proliferation in the presence of irradiated APC (1:1 ratio of APC:T cell); [CD3 mAb] shown, proliferation assessed at 72 h, representative of 3 independent experiments.

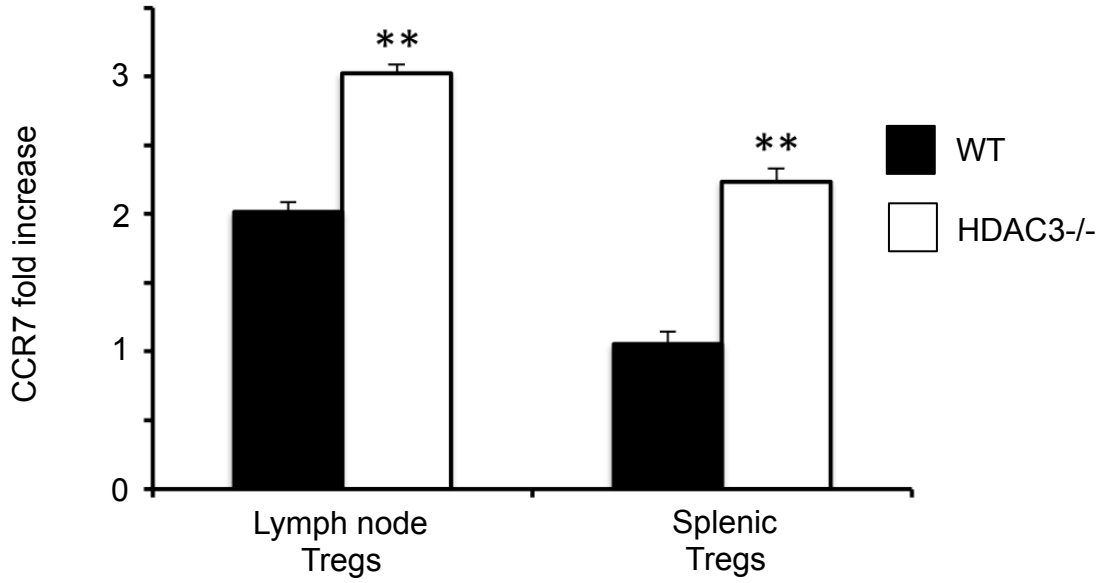

Suppl. Fig. 11 Effects of *Hdac3* deletion on CCR7 expression by lymph node and splenic Treg cells (qPCR, mean ± SD, 4/group, Student's t-test, **p<0.1 vs. WT).

Suppl. Table 1.

Histopathology of male versus female mice (aged 4 wks) with conditional deletion of *Hdac3* in their Treg cells[1]

Lung	Lungs demonstrate extensive perivascular and peribronchiolar inflammation primarily composed of mature lymphocytes and numerous neutrophils. The infiltrate predominantly involves large to medium-sized bronchovascular bundles with accentuation of bronchiolar-associated lymphoid tissue. The mixed inflammatory infiltrate also extends to involve distal airspaces with widening of intra-alveolar septae. The density of the inflammation is far higher in males compared to female mice.
Liver	Overall hepatic architecture is intact with mild to moderately dense lymphocytic infiltration involving the majority of large and small portal tracts. Inflammation is also present within the lobules and is focally associated with apoptotic hepatocytes. Inflammation is minimal to absent in livers from female mice.
Spleen	Splenic architecture is largely intact; however, peri-arteriolar lymphoid sheaths, while present, are small and poorly-organized. Extramedullary hematopoiesis characterized by numerous megakaryocytes and erythroid precursors are identified within the red pulp. Spleens from female mice show well-formed peri-arteriolar lymphoid sheaths.
Lymph nodes	Lymph nodes from male mice show effacement of normal nodal architecture, with loss of distinct follicles, and instead demonstrate scattered areas of lymphoid aggregates without well-formed germinal centers. Numerous histiocytes, some forming loose clusters are also scattered throughout the parenchyma. Lymph nodes from female mice show preservation of normal follicular architecture and minimal histiocytic infiltration.
Thymus	Male thymic tissues are atrophic with reduced lymphoid components and effacement of the cortico-medullary junctions, whereas female thymii appear normal.
Pancreas	Pancreatic parenchyma is normally formed with well-developed islets of Langerhans. Focal areas of extramedullary hematopoiesis are present predominantly within fibrous septae of the lobules.
Heart	Unremarkable cardiac myocytes.
Kidney	Renal parenchyma appears normally developed. No significant inflammatory infiltrate is identified.
Colon	Colonic mucosa shows intact villous architecture with no significant alterations in mucosal associated lymphoid tissue.

[1] H&E-stained paraffin sections of tissues from conditionally deleted mice were compared with features in littermate and WT controls (n=4-6/group).